Environmental Science & Technology

Article

Cite This: Environ. Sci. Technol. 2018, 52, 3275−3284

pubs.acs.org/est

Gasoline Particulate Filters as an Effective Tool to Reduce Particulate and Polycyclic Aromatic Hydrocarbon Emissions from Gasoline Direct Injection (GDI) Vehicles: A Case Study with Two GDI Vehicles

Jiacheng Yang,[†,‡] Patrick Roth,[†,‡] Thomas D. Durbin,[†,‡] Kent C. Johnson,[†,‡] David R. Cocker, III,[†,‡] Akua Asa-Awuku,[†,‡] Rasto Brezny,[§] Michael Geller,[§] and Georgios Karavalakis*[,†,‡]

[†]Bourns College of Engineering, Center for Environmental Research and Technology (CE-CERT), University of California, 1084 Columbia Avenue, Riverside, California 92507, United States

[‡]Department of Chemical and Environmental Engineering, Bourns College of Engineering, University of California, Riverside, California 92521, United States

[§]Manufacturers of Emission Controls Association, 2200 Wilson Boulevard, Suite 310, Arlington, Virginia 22201, United States

Supporting Information

ABSTRACT: We assessed the gaseous, particulate, and genotoxic pollutants from two current technology gasoline direct injection vehicles when tested in their original configuration and with a catalyzed gasoline particulate filter (GPF). Testing was conducted over the LA92 and US06 Supplemental Federal Test Procedure (US06) driving cycles on typical California E10 fuel. The use of a GPF did not show any fuel economy and carbon dioxide (CO_2) emission penalties, while the emissions of total hydrocarbons (THC), carbon monoxide (CO), and nitrogen oxides (NOx) were generally reduced. Our results showed dramatic reductions in particulate matter (PM) mass, black carbon, and total and solid particle number emissions with the use of GPFs for both vehicles over the LA92 and US06 cycles. Particle size distributions were primarily bimodal in nature, with accumulation mode particles dominating the distribution profile and their concentrations being higher during the cold-start period of the cycle. Polycyclic aromatic hydrocarbons (PAHs) and nitrated PAHs were quantified in both the vapor and particle phases of the PM, with the GPF-equipped vehicles practically eliminating most of these species in the exhaust. For the stock vehicles, 2−3 ring compounds and heavier 5−6 ring compounds were observed in the PM, whereas the vapor phase was dominated mostly by 2−3 ring aromatic compounds.

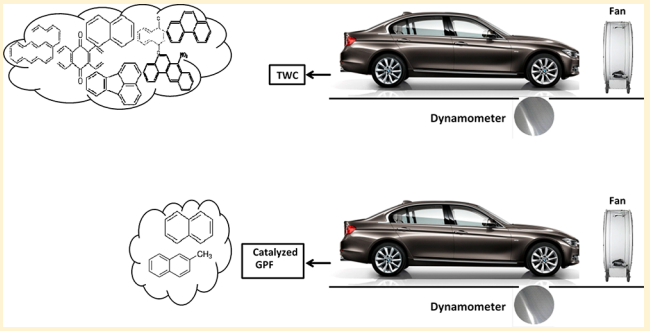

INTRODUCTION

Climate change has been attributed to an increase of anthropogenic greenhouse gas emissions, with the transportation sector being the largest contributor of carbon dioxide (CO_2) emissions.[1] Reducing CO_2 and other greenhouse gases is a key issue for regulatory agencies and industrial companies worldwide.[1] In the United States (U.S.), the Corporate Average Fuel Economy (CAFE) standards are currently very demanding for automotive manufacturers, with requirements to raise the average fuel economy of new cars and trucks to 54.5 miles per gallon by 2025. In the European Union (EU), similar mandates are set to decrease the CO_2 emissions to an average of 130 g/km. Because of the need to address global warming issues, gasoline direct injection (GDI) concepts have become the key technology of spark ignition (SI) engine development to reduce CO_2 emissions by improving the engine efficiency.[2]

Although GDI vehicles offer the potential of improved fuel economy, less fuel pumping, and charge air cooling, they tend to produce higher particulate matter (PM) emissions when compared with the traditional port fuel injection engines.[3−5] In GDI engines, fuel is sprayed directly into the combustion chamber, which leads to incomplete fuel evaporation due to the limited time available for fuel and air mixing, resulting in pockets with high temperatures but insufficient oxygen, leading to pyrolysis reactions and soot formation. Additionally, as the fuel comes directly into contact with the cold cylinder walls and piston, a small amount of fuel may impinge on the piston, which during evaporation may lead to diffusion combustion and PM formation.[3,6−8] The rapid market penetration of GDI vehicles has led governments to impose stricter standards to control PM emissions. California LEVIII and U.S. Tier 3 regulations began a four-year phase-in starting in 2015 and 2017, respectively, to a PM maximum of 3 mg/mile from the current 10 mg/mile LEVII limit. LEVIII will begin a four-year phase-in of a tighter 1 mg/mile starting in 2025. In the EU, the

Received: November 4, 2017
Revised: February 2, 2018
Accepted: February 15, 2018
Published: February 15, 2018

DOI: 10.1021/acs.est.7b05641
Environ. Sci. Technol. 2018, 52, 3275−3284

Euro 6a particle number (PN) standard for GDI vehicles was reduced from 6×10^{12} particles/km to 6×10^{11} particles/km in September 2017.

Meeting the strictest PM standard, of 1 mg/mile, and the European PN limit with GDI vehicles will likely be a challenge for automotive manufacturers. PM reductions in GDI platforms may be achieved by a combination of measures including alternative fuel formulations, fuel injection strategies, and the use of gasoline particulate filters (GPFs). Several studies have reported that the use of oxygenated fuels (i.e., ethanol) have generally beneficial impacts on PM emissions.[9−11] Other studies have shown that centrally mounted injection systems have lower mass and number emissions than wall-guided injection systems because the injector is located close to the spark plug, leading to better fuel evaporation and less wall-wetting effects.[11,12] The use of GPFs in GDI vehicles may still be needed to meet future tightened regulations, and an increasing number of studies are focusing in this research area.[13−15] This is particularly true for the EU where the strict PN emissions standard for diesel particulate filter (DPF) equipped diesel vehicles was essentially translated to GDI vehicles. The stringent PN limit combined with the Real Driving Emissions (RDE) requirements that came into effect with Euro 6c has led to numerous OEMs reporting wide deployment of GPFs across their new vehicle fleets. Mamakos et al.[16] showed that the installation of GPFs in GDI vehicles is both feasible and cost-effective. In a different study, Mamakos and co-workers[17] reported that GPFs had filtration efficiencies in excess of 89% for PN emissions for a Euro 6 technology GDI vehicle over the New European Driving Cycle (NEDC) and the Common Artemis Driving Cycle (CADC). Chan et al.[18] also showed large reductions in black carbon and solid particle number (SPN) emissions with the use of a GPF with a GDI vehicle tested over the U.S. Federal Test Procedure (FTP) and the US06 Supplemental Federal Test Procedure (SFTP or US06) cycles. Choi et al.[19] reported lower PN emissions for a GPF-equipped GDI vehicle in another study, but the filtration efficiency of 57% was lower than what has previously been reported in studies.[17,18,20]

It is important to better understand the toxicity of the particles being formed in GDI combustion. Today, the literature is scarce about the toxic properties of PM emissions from GDI vehicles, such as those of polycyclic aromatic hydrocarbons (PAHs) and their oxygenated (oxy-PAHs) and nitrated derivatives (nitro-PAHs).[21,22] PAHs have long been recognized as one of the major soot precursors for soot particles, while they are also classified as carcinogenic and mutagenic compounds adsorbed onto the PM or partition in the semivolatile PM phase.[23,24] Additionally, some oxy-PAH and nitro-PAH species have been recognized as similarly or more toxic than their parent PAHs.[25]

This study aims to better characterize the toxicity of PM from GDI vehicles and the potential for catalyzed GPFs to reduce this toxicity. This study assessed the PM mass and particle number (PN) emissions and chemical constituents, such as PAHs and nitro-PAHs, in the particle and vapor phases of exhaust from two current technology GDI vehicles tested in their original configuration and when equipped with GPFs. The vehicles were tested over the LA92 and US06 test cycles on a chassis dynamometer, with the resulting exhaust samples being characterized for toxic species. The emissions results will be presented and discussed in the context of the influences of driving conditions, aftertreatment system, and engine technology.

EXPERIMENTAL SECTION

Test Vehicles and Driving Cycles. This study utilized two 2016 model year passenger cars. GDI_1 was equipped with a 2.0 L wall-guided direct injection SI Atkinson cycle engine, and GDI_2 was equipped with a 1.5 L downsized turbocharged centrally mounted direct injection engine. Both vehicles were operated stoichiometrically and were equipped with three-way catalysts (TWCs). GDI_1 and GDI_2 were certified to meet LEV III SULEV30 (PZEV) and LEV II emissions standards and had 14 780 and 24 600 miles at the start of the campaign, respectively.

After the baseline emissions were measured, both vehicles were retrofitted with a catalyzed GPF installed in place of the underfloor TWC. The original close-coupled catalysts were retained in their stock location. The catalyzed GPFs were provided by the Manufacturers of Emissions Controls Association (MECA). The GPFs were sized based on the engine displacement of each vehicle, and they were catalyzed with precious metal loadings typical of underfloor catalysts matching the certification levels of the two vehicles. Both GPFs were 4.66 in. in diameter and 4.5 in. in length, with an 8 mil cell wall thickness and a cell density of 300 cells per square inch (cpsi). The GPFs had a TWC washcoat with approximately 1.0 g/L loading of palladium (Pd) and rhodium (Rh) (Pd:Rh ratio of 4:1).

Both vehicles were tested over duplicate LA92s and US06 cycles on typical California E10 fuel. The LA92 test cycle or the California Unified Cycle (UC) is a dynamometer driving schedule for light-duty vehicles developed by the California Air Resources Board (CARB). The LA92 consists of three phases (i.e., cold-start, urban, and hot-start phases) and has a three-bag structure similar to the FTP cycle. The LA92 is characterized by higher speeds, higher accelerations, fewer stops per mile, and less idle time than the FTP. The US06 was developed to reflect aggressive, high speed, and high acceleration driving behavior. Unlike the LA92, it is a hot-start test typically run with a prep cycle to ensure the vehicle is warmed up. For this study, two US06 preconditioning cycles followed by a 10 min soak period were performed as prep prior to conducting the actual US06 emission test cycles.

Emissions Testing. All tests were conducted in CE-CERT's Vehicle Emissions Research Laboratory (VERL), on a Burke E. Porter 48 in. single-roll electric dynamometer. A Pierburg positive displacement pump-constant volume sampling (PDP-CVS) system was used to obtain standard bag measurements for total hydrocarbons (THC), carbon monoxide (CO), nitrogen oxides (NO_x), nonmethane hydrocarbons (NMHC), and carbon dioxide (CO_2). Bag measurements were made with a Pierburg AMA-4000 bench. PM mass, total and solid PN, particle size distributions, elemental and organic carbon (EC/OC) fractions, and black carbon emissions were also measured. Total and solid particles were counted with a TSI 3776 ultrafine CPC and downstream of a catalytic stripper with a TSI 3776 ultrafine CPC, respectively, where both were connected to an ejector diluter that was used to collect samples from the CVS tunnel. Solid particle counts were also measured in the raw exhaust before the CVS with a TSI NPET 3795 to evaluate the filtration efficiencies of the GPFs. Detailed information on the methods used to collect and analyze these emissions is provided in the Supporting Information. Analyses of PAH and nitro-

DOI: 10.1021/acs.est.7b05641
Environ. Sci. Technol. 2018, 52, 3275−3284

Table 1. Regulated Emissions and Fuel Economy, Expressed in Grams Per Mile and Miles Per Gallon, Respectively, over the LA92 and US06 Cycles

	GDI_1	GDI_1/GPF	GDI_2	GDI_2/GPF
		LA92 Cycle		
THC	0.010 ± 0.001	0.006 ± 0.001	0.062 ± 0.003	0.024 ± 0.001
NHMC	0.008 ± 0.001	0.005 ± 0.001	0.054 ± 0.003	0.019 ± 0.001
CO	0.189 ± 0.017	0.141 ± 0.043	0.665 ± 0.038	0.195 ± 0.010
NO_x	0.010 ± 0.001	0.008 ± 0.000	0.066 ± 0.003	0.008 ± 0.001
CO_2	271.3 ± 13.7	254.2 ± 0.7	339.2 ± 2.5	330.7 ± 11.0
fuel economy	31.8 ± 1.6	33.9 ± 0.1	25.3 ± 0.2	26.0 ± 0.8
		US06 Cycle		
THC	0.007 ± 0.000	0.006 ± 0.003	0.040 ± 0.002	0.008 ± 0.002
NHMC	0.005 ± 0.000	0.004 ± 0.002	0.029 ± 0.001	0.002 ± 0.001
CO	0.235 ± 0.332	0.225 ± 0.184	4.210 ± 0.462	1.456 ± 0.213
NO_x	0.002 ± 0.003	0.007 ± 0.005	0.138 ± 0.008	0.004 ± 0.000
CO_2	248.1 ± 3.4	243.8 ± 21.0	334.9 ± 1.2	340.0 ± 0.8
fuel economy	34.8 ± 0.5	35.5 ± 3.0	25.3 ± 0.1	25.2 ± 0.0

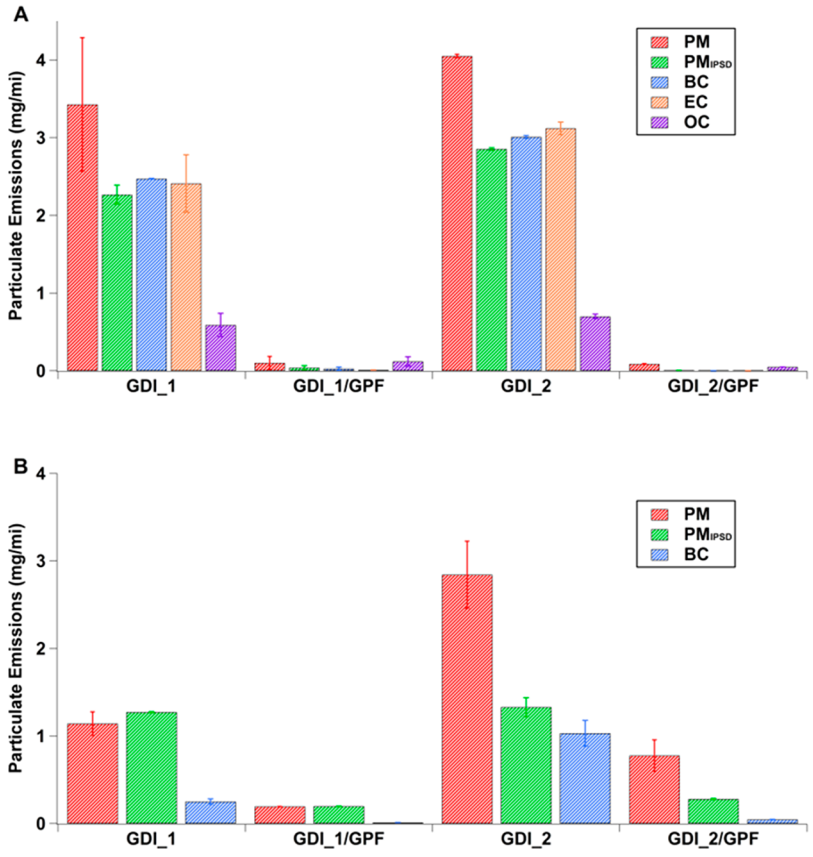

Figure 1. Gravimetric PM mass, PM mass calculated based on the IPSD method, black carbon, and EC/OC emissions over the LA92 cycle (a) and gravimetric PM mass, PM mass calculated based on the IPSD method, and black carbon emissions over the US06 cycle for both vehicles (b).

PAH species were performed at the Desert Research Institute, Reno, NV. PAH and nitro-PAH samples were collected on precleaned Teflon-impregnated glass fiber (TIGF) filters (100 mm). Semivolatile organic compounds were collected on cleaned Amberlite XAD-4 polyaromatic absorbent resin (Aldrich Chemical Co., Inc.) that was packed into a glass cartridge. The samples collected on each filter-XAD sampling train were extracted separately with high-purity dichloromethane and then acetone, followed by an accelerated solvent extraction (ASE). A Varian 4000 Ion Trap in electron impact (EI) mode was used for PAH analysis, and a Varian 1200 triple quadrupole GC/MS operating in negative chemical ionization (CI) mode was used for nitro-PAH compounds. Negative CI offers superior sensitivity for the analysis of nitro-PAHs (approximately 100 times higher than EI or positive CI) and other compounds with electron-withdrawing substituents, but not for regular PAH and hydrocarbons. More details on the analysis methods of PAH and nitro-PAH compounds can be found elsewhere.[26]

RESULTS AND DISCUSSION

Gaseous Emissions and Fuel Economy. Table 1 shows the gas-phase emissions and fuel economy results for the two GDI vehicles with and without the GPFs. The installation of

DOI: 10.1021/acs.est.7b05641
Environ. Sci. Technol. 2018, 52, 3275−3284

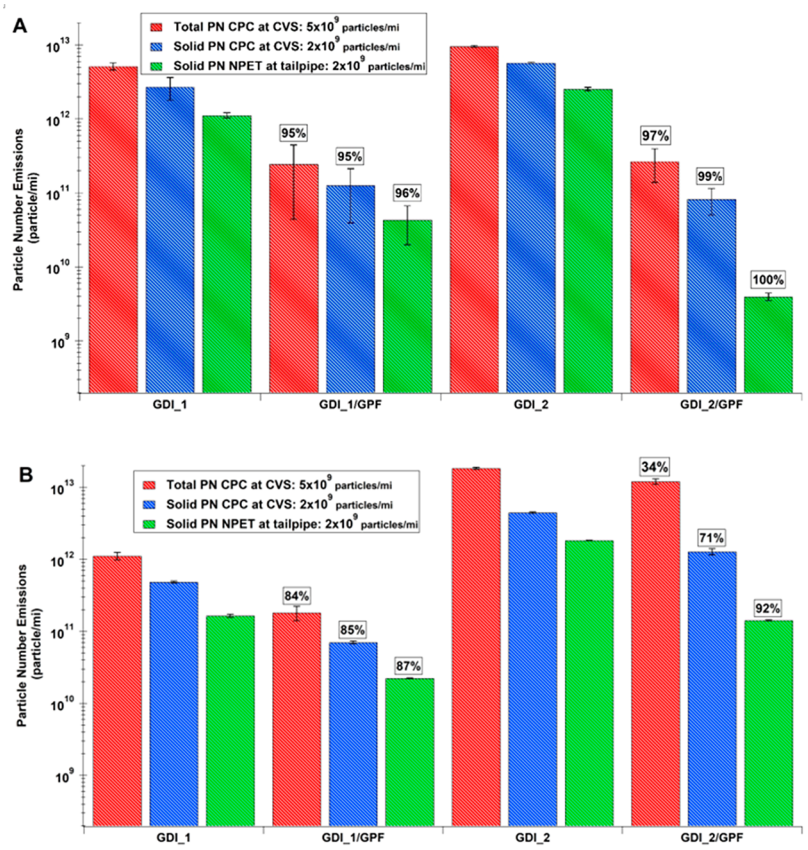

Figure 2. Total and solid particle number emissions over the LA92 cycle (a) and US06 cycle (b) for both test vehicles.

the catalyzed GPFs into the exhaust systems for both GDI vehicles led to some differences in the regulated emission levels and fuel economy, as shown in Table 1. A clear reduction was observed for CO, THC, NMHC, and NOx emissions with the use of GPFs over both the LA92 and US06 cycles. Spiess et al.[20] and Xia et al.[27] also showed gas-phase emission improvements with the use of a catalyzed GPF, especially for NOx emissions. The reductions in THC, CO, and NOx emissions over the LA92 cycle with the catalyzed GPFs compared to the stock configuration were 37%, 26%, and 17% for GDI_1 and 62%, 71%, and 88% for GDI_2. NOx, THC, and CO conversion occurs mainly on the TWC. It appeared that the catalyzed GPFs, which have TWC coatings and precious metal loadings similar to the original underfloor converter, provided additional catalytic active surface, which enhanced the conversion of NOx, THC, and CO emissions. For the cold-start phase of LA92, the reductions in emissions with the GPFs compared to the stock configuration emission levels were not as pronounced because of the catalyst being below its light-off temperature (Table S1). A small, but statistically significant, increase in CO_2 emissions was seen for the GDI_2/GPF configuration compared to GDI_2 without the GPF, although there were no statistically significant differences in fuel economy between these two configurations. This can be attributed to the greater oxidation of CO emissions to CO_2 for the GPF configuration. CO_2 emissions and fuel economy did not show statistical differences between the stock and GPF equipped vehicles for the other cases.

PM Mass, Black Carbon, and Particle Number Emissions. Figure 1a,b shows the PM mass, organic carbon (OC) and elemental carbon (EC) fractions, and black carbon emissions for both vehicles over the LA92 and US06 cycles. PM mass emissions were lower for the wall-guided GDI_1 vehicle compared to the centrally mounted GDI_2 vehicle. This was likely due to the higher compression ratio for GDI_1 (14.0:1) compared to GDI_2 (10.0:1), which probably resulted in an earlier fuel injection, leading to the formation of a more homogeneous air−fuel mixture due to the availability of sufficient time for mixture preparation, as well as the higher in-cylinder temperature, which increased the oxidation of particles in the combustion chamber, resulting in lower PM emissions for GDI_1. It also has to be noted that GDI_1 is certified to more stringent LEV III standards compared to GDI_2, which is certified to a LEV II standard. Vehicle weight, engine size, and calibration strategy can play a role in PM emissions. PM mass and black carbon emissions were drastically reduced with the GPFs, with these reductions being on the order of 97% and 99% for GDI_1/GPF and 98% and 100% for GDI_2/GPF on the LA92 and US06 cycles, respectively. Previous chassis dynamometer studies also showed reductions in PM mass from GDI vehicles with the use of GPFs.[17−19,28]

PM mass emissions were also calculated using the integrated particle size distribution (IPSD) method, which is an alternative metric for measuring PM mass from real-time mobility-based particle size distributions that are converted into mass distributions by applying a size-resolved particle effective density, as shown in previous studies.[29,30] The PM mass reduction based on the IPSD method was 34% and 30% for GDI_1 and GDI_2 and 60% and 94% for GDI_1/GPF and GDI_2/GPF, respectively, lower than the gravimetric PM mass over the LA92 but similar to the black carbon or soot emissions

DOI: 10.1021/acs.est.7b05641
Environ. Sci. Technol. 2018, 52, 3275−3284

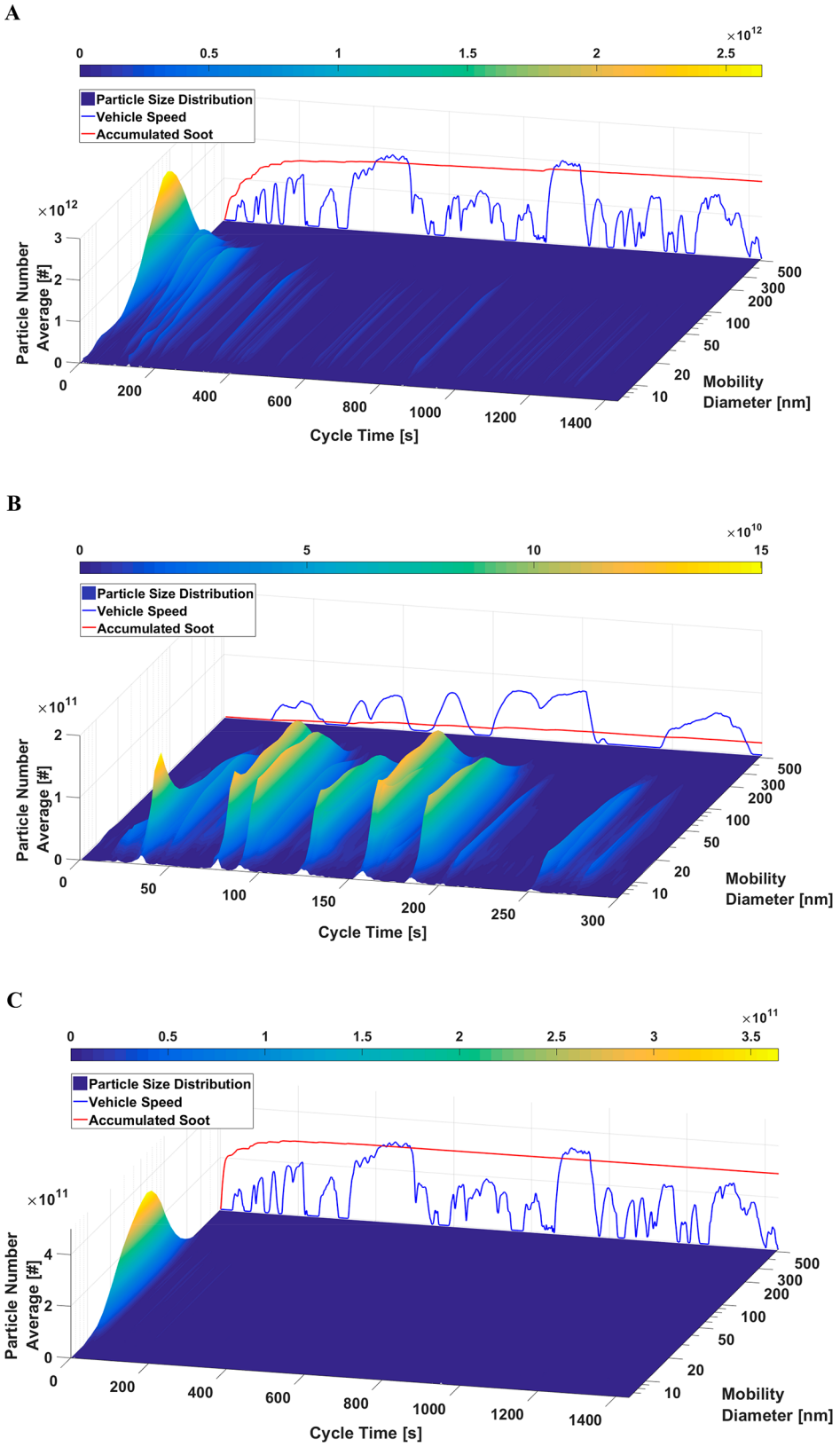

Figure 3. Transient particle size distribution for phases 1 and 2 of the LA92 for GDI_1 (a); particle size distribution for phase 3 of the LA92 for GDI_1 (b); and particle size distribution for phases 1 and 2 of the LA92 for GDI_1/GPF (c). The speed-time profile and the accumulated soot mass are also included for visual reference

(Figure 1a). The underestimation for the IPSD method compared to the gravimetric PM mass implies that most of the PM was EC or black carbon in nature and that the semivolatile components of PM were not taken into account with the IPSD measurement. These components can condense onto the filters collecting PM mass but are not be measured by

DOI: 10.1021/acs.est.7b05641
Environ. Sci. Technol. 2018, 52, 3275−3284

the IPSD method. For the US06 cycle, the IPSD method agreed well with the gravimetric PM mass for GDI_1 but underestimated the gravimetric PM mass for GDI_2. The PM mass composition from both vehicles was dominated by EC, as confirmed by the black carbon emission measurements, whereas OC constitutes only a small fraction of PM. However, when both vehicles were retrofitted with the GPFs, the OC fraction was found to be higher than the EC fraction of the PM. The GPFs proved capable of eliminating most of the black carbon or soot particles but not all of the semivolatile organic compounds.

Total and solid (>23 nm) PN emissions are shown in Figure 2a. For both vehicles, total and solid PN counts are in line with the gravimetric PM mass. The cold-start phase of the LA92 cycle generated significantly higher PN emissions than the hot-running and hot-start phases, because of incomplete combustion, as shown by the THC emissions (Table S1), and liquid fuel impingement onto the cold piston bowl and cylinder surfaces.[8] As expected, PN emissions during hot-start operation were markedly lower because of the increased fuel temperature and temperature of the engine parts that promote almost complete fuel vaporization and better fuel−air mixing. The use of GPFs resulted in larger reductions for both total and solid PN emissions; for GDI_1/GPF, the filtration efficiencies were 95% for both total and solid PN, while for GDI_2/GPF the filtration efficiencies were 97% for total PN and 99% for solid PN. Interestingly, both total and solid PN emissions for the stock and GPF-equipped vehicles are of similar magnitude, suggesting that most of the emitted particles were solid in nature with diameters larger than 23 nm.

Total and solid PN emissions over the US06 are shown in Figure 2b. For GDI_1/GPF, the reductions in total and solid PN were 83% and 85%, respectively, compared to 34% and 71% for GDI_2/GPF. Solid particle counts measured in the raw exhaust significantly decreased with the use of GPFs, indicating filtration efficiencies in the range of 86%−92% for both vehicles. It is theorized that the low reductions in PN emissions when measured with the TSI CPCs for GDI_2/GPF were an artifact of potential CVS and exhaust transfer line contamination. GDI_2/GPF systematically showed higher exhaust and CVS inlet temperatures than GDI_1/GPF, as shown in Figure S1. The high-speed and high-load driving conditions for the US06, coupled with temperatures above 250 °C for more than 10 min, will likely lead to the desorption or pyrolysis of stored volatile and solid particles, as well as other organic material by the hot exhaust gases from the exhaust transfer line and the CVS tunnel surfaces. This phenomenon has also been observed previously in studies using the US06 cycle.[31]

Particle Size Distributions. Average particle size distributions are illustrated in Figure 3 for GDI_1 and in Figure S2 for GDI_2. The particle size distribution profile for GDI_1 was bimodal in nature with accumulation or soot mode particles dominating over nucleation mode particles. Particle populations were centered in the accumulation mode between 40 and 120 nm in diameter. Similar particle size distribution profiles with higher concentrations of accumulation mode particles and a much smaller nucleation mode from GDI vehicles have been shown in other studies.[32,33] The cold-start emissions during the first 200 s represent a significant fraction of the total emitted particles over the entire LA92 cycle, especially for GDI_1 (Figure 3a). For GDI_2, high levels of accumulation mode particles were seen for a longer duration of phase 1, up to 400 s. During cold-start operation, a significant portion of the injected fuel lands on the cold combustion chamber surfaces. Because the combustion chamber walls are at lower temperature than the saturation temperature of most of the species of the injected fuel, the result is the formation of fuel films that fail to evaporate completely, creating overly fuel-rich zones that are responsible for the high levels of particle emissions during cold-start.[6,34] Typically, cold-start operation favors the formation of accumulation mode particles consisting of carbonaceous chain agglomerates.[35] The cold fuel can lead to poor fuel vaporization and mixture deficiencies resulting in pool fires and diffusive combustion and the formation of soot particles in the accumulation mode.[3,35,36] It is clear that after 250−300 s the particle concentrations were drastically reduced because of the warm-up of the engine and exhaust surfaces. Overall, the drops in particle size and concentrations were likely due to better fuel vaporization, less wall wetting, and avoidance of pool fires. Sharp reductions were also observed for the nucleation mode particles for both vehicles after the first 400 s. It is assumed that the TWC was above its light-off temperature and thus capable of oxidizing volatile organic hydrocarbons from unburned fuel that primarily constitute the nucleation mode.

The hot-start particle concentrations for both vehicles were about an order of magnitude lower compared to cold-start emissions (Figure 3b). For GDI_1, the nucleation mode was prominent for phase 3 compared to phases 1 and 2 of the LA92, with the particle size distribution being bimodal and trimodal in nature. In contrast, GDI_2 showed a dominance of accumulation mode particles and practically the absence of a nucleation mode during hot-starts. The results reported here for the GPF-equipped vehicles showed particle concentrations orders of magnitude lower than the stock vehicles for all phases of the LA92. In fact, only cold-start showed some spikes of accumulation mode particles for GDI_1/GPF (Figure 3c), whereas hot-start emissions were at the noise level of the measurement. Similarly, GDI_2/GPF showed larger peaks for nucleation mode particles but at very low concentrations and close to the noise levels (Figure S4).

The particle size distributions for both vehicles over the US06 cycles are shown in Figures S5a,b and S6a,b. The particle size distributions for the US06 are vehicle-dependent and exhibited substantial differences compared to the LA92 cycle, with the majority of the particle populations centered in the nucleation mode. There was a shift of the accumulation mode toward smaller-diameter particles for GDI_1, while the accumulation mode disappeared leaving the nucleation mode dominating the particle sizing profile for GDI_2. For GDI_1, the nucleation and soot particle number concentrations were lower for the GPF configuration as they were more effectively removed by the GPF. For GDI_2, a burst of nucleation mode particles was observed for both configurations. Previous studies have shown elevated particle number emissions over US06 operation, suggesting a possible filter regeneration event.[37] As previously discussed, the higher nucleation particle populations with the GPF were attributed to CVS contamination issues from hydrocarbon deposits on the walls rather than GPF regeneration mechanisms, as shown elsewhere.[38] These hydrocarbon deposits and other organic material will likely lead to particle nucleation in the dilution tunnel.[31] Maricq et al.[39] also showed significant nucleation mode exhaust particle emissions from GDI vehicles during US06 operation, which was associated with sulfate promoting semivolatile hydrocarbons to nucleate instead of condensing onto soot particles.

DOI: 10.1021/acs.est.7b05641
Environ. Sci. Technol. 2018, 52, 3275−3284

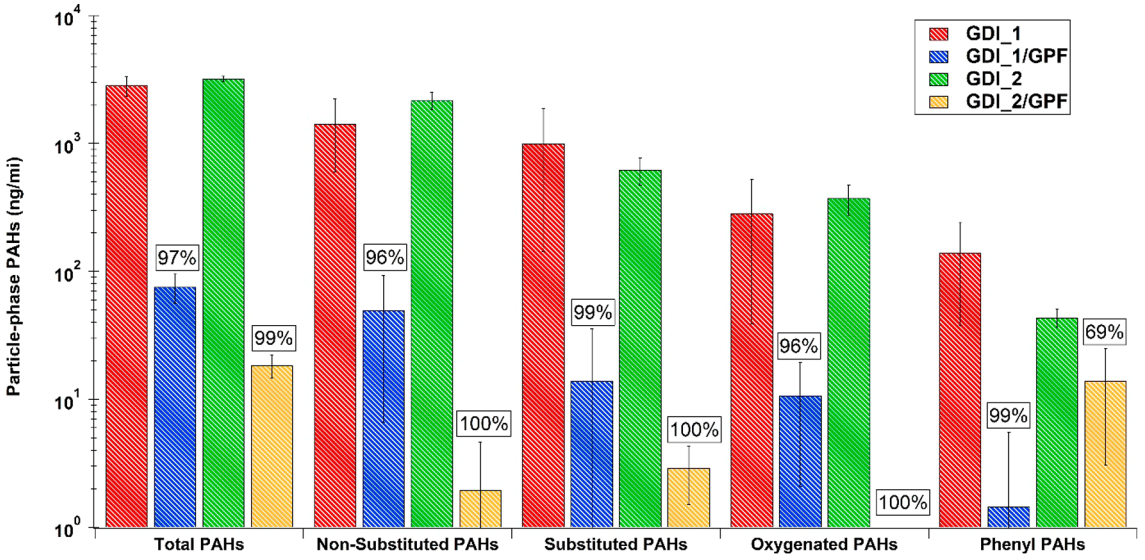

Figure 4. Total particle-phase PAH emissions for both test vehicles over the LA92 cycle.

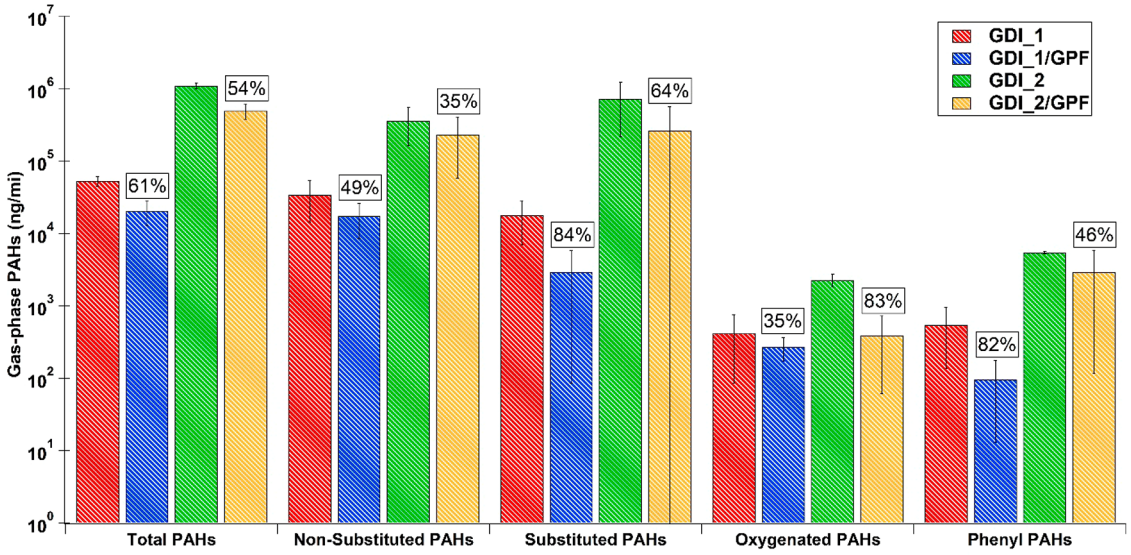

Figure 5. Total gas-phase PAH emissions over the LA92 cycle.

PAH and Nitro-PAH Emissions. Emissions of particle- and vapor-phase PAHs categorized by families of compounds for substituted, nonsubstituted, oxygenated, and phenyl PAHs are shown in Figures 4 and 5, respectively. The individual particle- and vapor-phase PAH compounds are listed in Tables S2 and S3. Particle-phase PAH emissions showed large overall reductions with the application of GPFs for both vehicles, which were on the order of 97% and 99% for GDI_1/GPF and GDI_2/GPF, respectively. The GPFs practically eliminated PAH emissions in the particle phase, with their levels being below the detection limit. For the stock vehicles, 2−3 member ring compounds dominated the distribution of PAHs, with lower levels of high molecular weight species. Higher concentrations of heavier PAHs with up to 6 rings were detected in the exhaust of GDI_2 compared to GDI_1. Compounds like methyl-pyrenes, methyl-phenanthrenes, benzo(*ghi*)fluoranthene, benzo(*a*)pyrene, indeno[123-*cd*]-pyrene, coronene, etc., were found in significantly higher levels in GDI_2 exhaust than GDI_1. This is in agreement with the higher PM mass of this vehicle, because PAHs with four or more fused rings play an important role in contributing to PM mass formation.[40] Interestingly, total particle-phase PAH emissions for the stock GDI_2 were higher than the stock GDI_1, whereas GDI_2/GPF showed much lower total particle-phase PAH emissions relative to GDI_1/GPF, indicating a higher filtration efficiency for this vehicle. It should be stressed that the PAH species (benzo(*a*)pyrene, benzo(*a*)-anthracene, benzo(*b*)fluoranthene, benzo(*k*)fluoranthene, chrysene, dibenzo(*a,h*)anthracene, benzo(*ghi*)perylene, and indeno(1,2,3-*cd*)pyrene) are considered to be carcinogenic and toxic to humans by the International Agency for Research on Cancer (IARC) and the U.S. EPA, and they were found in relatively high concentrations in the particle phase.[41] Some of the heavier PAHs seen in the present experiment were also observed in a previous chassis dynamometer study using a GDI vehicle.[42] Although benzo(*a*)pyrene is considered a Class 1 carcinogen by the IARC, other heavier PAHs such as dibenzo(*a,h*)pyrene possess a carcinogenic potential about 10 times higher than that of benzo(*a*)pyrene.[43] These findings suggest that GDI exhaust could possess high potency due to the

DOI: 10.1021/acs.est.7b05641
Environ. Sci. Technol. 2018, 52, 3275−3284

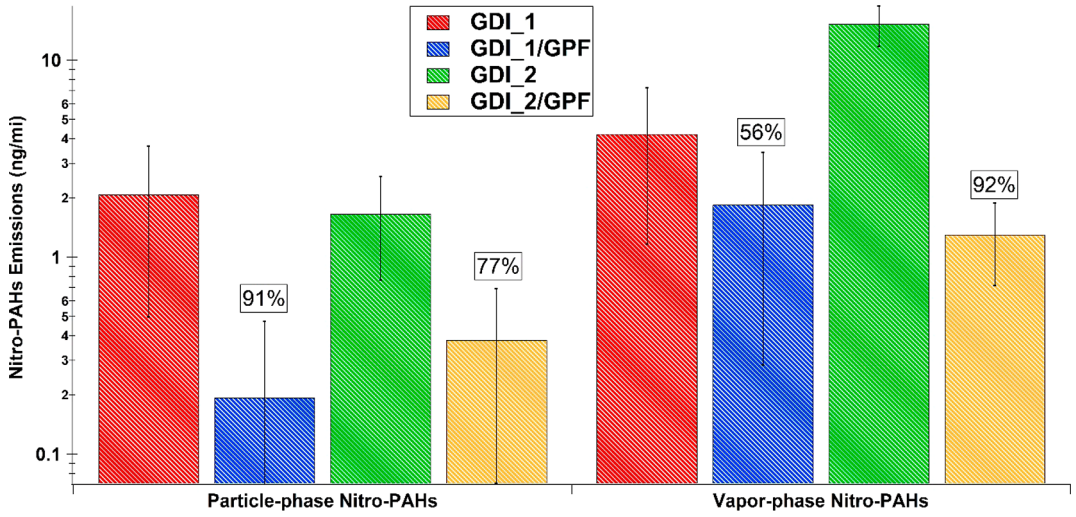

Figure 6. Total particle- and gas-phase nitrated PAH emissions for both test vehicles over the LA92 cycle.

presence of heavier PAH emissions, even at low concentrations in the sample.

It should be noted that both vehicles presented a diverse profile in their PAH distribution, with light, medium, and heavier molecular weight PAHs being abundant in the exhaust. In the absence of oxygen and at temperatures above 400 °C, the hydrocarbon molecules from the fuel or lubricating oil are decomposed into smaller active radicals (H, OH, CH_3, C_2H_4, C_2H_2) that form PAH molecules.[44,45] Lighter and medium molecular weight PAHs, such as phenanthrene, fluoranthene, and pyrene, were likely sourced from pyrosynthesis routes of *n*-alkanes in the fuel through reactions of naphthalene and indene with acetylene (hydrogen abstraction C_2H_2 addition, HACA mechanism) or cyclopentadienyl.[46] Heavier PAHs, such as benzo(a)pyrene, benzo(*b*+*j*+*k*)fluoranthene, benzo(*a*)-anthracene, benzo(*ghi*)fluoranthene, indeno[123-*cd*]pyrene, and coronene, could be attributed to the pyrolysis from the incomplete combustion of larger fuel fragments and the lubricant oil.[21] In GDI engines, the lubricating oil can penetrate the combustion chamber either via the cylinder walls or via the intake ports and contribute to PM and PAH formation, primarily because of its higher evaporation temperature that results in incomplete vaporization. Noncombusted PAHs from fuel pyrolysis condense and accumulate in the lubricating oil, which acts as a sink for PAHs.[47]

As shown in Figure 4, the total particle-phase PAHs by category showed the following distribution for both vehicles: nonsubstituted > substituted > oxygenated > phenyl. Naphthalene was the predominant nonsubstituted PAH compound in the particle phase for both vehicle configurations, followed by phenanthrene, fluoranthene, pyrene, benzo(*ghi*)-fluoranthene, benzo(*b*+*j*+*k*)fluoranthene, and others. These PAH species were likely produced from the thermal cracking of fuel directly injected into the cylinder. For the substituted PAH emissions, methyl-, dimethyl-, and trimethyl-naphthalenes; methyl- and dimethyl-phenanthrenes; and methyl-pyrenes were the dominant compounds in the exhaust. The predominant particle-phase oxy-PAH compounds for both vehicles were 9-fluorenone, perinaphthenone, anthraquinone, and dibenzofuran. While the stock GDI_2 had the highest total oxy-PAH concentrations, the addition of the GPF eliminated these species from the exhaust. For the total phenyl PAH emissions, GDI_1 showed higher concentrations relative to GDI_2, with biphenyl being the dominant species in the exhaust.

The total vapor-phase PAH emissions were found in significantly higher concentrations than the particle-phase emissions, with GDI_2 showing higher concentrations of tailpipe vapor-phase PAHs than GDI_1. The predominantly semivolatile PAHs were mainly those with two and three-member rings, with a small amount of four-member ring PAHs. Heavier PAHs of four or more rings were predominantly adsorbed in the particle (soot) phase. Naphthalene was the largest contributor to the total vapor-phase PAHs, followed by methyl-, ethyl-, and dimethyl-naphthalene. Unlike for the particle-phase PAHs, where total PAH emissions decreased by more than 97% with the GPF addition, the reductions in the vapor phase were generally lower. Specifically, the reductions for the total vapor-phase substituted, nonsubstituted, oxygenated, and phenyl PAHs emissions were 84%, 49%, 35%, and 82% for GDI_1/GPF, while for GDI_2/GPF they were 64%, 35%, 83%, and 46%, respectively. These results suggest that PAHs existing in the vapor-phase are not eliminated by the GPF as effectively as those associated with the particle-phase over the LA92 cycle. It has to be noted that substantial reductions of vapor-phase PAHs with a GPF are not expected; however, the catalyzed GPFs provided the additional catalytically active coating resulting in the partial oxidation of the vapor-phase PAH species.

Particle-phase nitro-PAH emissions were found in much lower concentrations than their parent PAHs, as shown in Figure 6 and in Tables S4 and S5. The reductions in total nitro-PAH emissions were 91% and 77% for GDI_1/GPF and GDI_2/GPF, respectively. For the stock vehicles, the most prevalent nitro-PAH species in the particle phase were 1-nitronaphthalene, 2-nitronaphthalene, 9-nitroanthracene, 1-nitropyrene, 2-nitrofluoranthene, and 2,7-dinitrofluorene. Although the emissions of the most volatile two-ring species were higher than those of the three- and four-ring nitro-PAHs for GDI_1, some heavier nitro-PAHs for GDI_2, such as 2-nitrofluoranthene and 2,7-dinitrofluorene, showed higher emissions than the lighter nitronaphthalenes. Interestingly, some species were detected only for both vehicles with the GPFs, suggesting that these nitro-PAHs formed de novo in the GPF system via selective nitration reactions. Similar to the parent PAHs, the vapor-phase nitro-PAH emissions were seen

DOI: 10.1021/acs.est.7b05641
Environ. Sci. Technol. 2018, 52, 3275−3284

in higher concentrations than the particle-phase emissions. The reductions in total vapor-phase nitro-PAH emissions with the use of GPF were 56% and 92% for GDI_1 and GDI_2, respectively. The lighter two-member ring species of 1-nitronaphthalene and 2-nitronaphthalene were the most dominant in the exhaust followed by 1-methyl-6-nitronaphthalene and 9-nitroanthracene. The compounds of 1-nitropyrene and 4-nitropyrene were also found in the vapor phase, with both being four-member ring species that usually exist in the particle phase. 1-Nitropyrene is both toxic and mutagenic, while nitropyrenes are generally precursors for the more potent and mutagenic dinitropyrenes.[48]

Implications. Our results demonstrate that current technology GDI vehicles could be an important source for on-road ultrafine particles and black carbon emissions and ultimately a contributor to urban air pollution. This study revealed that catalyzed GPFs can improve the conversion efficiency for NOx, THC, and CO emissions and have no measurable impact on CO_2 emissions and fuel economy. This is one of the few studies revealing that GDI vehicles could significantly contribute to PAH and nitrated PAH emissions and to our knowledge the only one that looked at remediation of these toxic species using a catalyzed gasoline particulate filter. We found that the use of catalyzed GPFs could significantly reduce the PM mass and black carbon emissions, as well as total and solid particle number emissions, without having a measurable impact on the vehicle's GHG emissions and fuel economy. The catalyzed GPF significantly reduced the particle-phase PAHs and nitro-PAHs emissions, especially the less volatile or highly reactive PAH species. On the other hand, the vapor-phase PAHs did not show the same filtration efficiency as the PM-bound compounds. This study showed that GDI vehicle exhaust is characterized by a diverse PAH distribution profile, ranging from 3 to 6 ring species. The projected increased penetration of GDI vehicles in the U.S. market suggests that future health studies aimed at characterizing the toxicity of GDI emissions are needed to understand the health risks associated with non-GPF-equipped GDI PM emissions. The fact that GPF adoption from U.S. vehicle manufacturers is not as dynamic as in the EU, because of the more stringent European PN standard especially over real-driving emissions (RDE) testing, should raise concerns about the lack of societal and air quality benefits from the GDI fleet.

■ ASSOCIATED CONTENT

Supporting Information

The Supporting Information is available free of charge on the ACS Publications website at DOI: 10.1021/acs.est.7b05641.

Further details on the experimental procedures and protocols, emissions methods analyses, and emissions results (PDF)

■ AUTHOR INFORMATION

Corresponding Author

*Phone: (951)-781-5799; fax: (951)-781-5790; e-mail: gkaraval@cert.ucr.edu.

ORCID

Akua Asa-Awuku: 0000-0002-0354-8368

Georgios Karavalakis: 0000-0001-5011-8371

Notes

The authors declare no competing financial interest.

■ ACKNOWLEDGMENTS

The authors thank Mr. Mark Villela and Mr. Daniel Gomez of the University of California, Riverside for their contribution in contacting this research program. We also thank MECA for providing the catalyzed GPF for this program and also for their technical support and guidance. We acknowledge funding from the South Coast Air Quality Management District (SCAQMD) under contract 15625 and the Manufacturers of Emission Controls Association (MECA) under contract 15040420.

■ REFERENCES

(1) Pachauri, R. K.; Reisinger, A. *IPCC 2007: Climate Change 2007: Synthesis report. Contribution of Working Groups I, II, and III to the Fourth Assessment Report of the Intergovernmental Panel on Climate Change*; IPCC: Geneva, Switzerland, 2007.

(2) Alkidas, A. C. Combustion advancements in gasoline engines. *Energy Convers. Manage.* **2007**, *48*, 2751−2761.

(3) Piock, W.; Hoffmann, G.; Berndorfer, A.; Salemi, P.; Fusshoeller, B. Strategies towards meeting future particulate matter emission requirements in homogeneous gasoline direct injection engines. *SAE Int. J. Engines* **2011**, *4*, 1455−1468.

(4) Karavalakis, G.; Short, D.; Vu, D.; Russell, R.; Hajbabaei, M.; Asa-Awuku, A.; Durbin, T. D. Evaluating the effects of aromatics content in gasoline on gaseous and particulate matter emissions from SI-PFI and SI-DI vehicles. *Environ. Sci. Technol.* **2015**, *49*, 7021−7031.

(5) Su, J.; Lin, W.; Sterniak, J.; Xu, M.; Bohac, S. V. Particulate matter emission comparison of spark ignition direct injection (SIDI) and port fuel injection (PFI) operation of a boosted gasoline engine. *J. Eng. Gas Turbines Power* **2014**, *136*, 091513.

(6) Stevens, E.; Steeper, R. Piston wetting in an optical DISI engine: Fuel films, pool fires, and soot generation. *SAE Tech. Pap. Ser.* **2001**, 2001-01-1203.

(7) Karlsson, R. B.; Heywood, J. B. Piston fuel film observations in an optical access GDI engine. *SAE Tech. Pap. Ser.* **2001**, 2001-01-2022.

(8) He, X.; Ratcliff, M. A.; Zigler, B. T. Effects of gasoline direct injection engine operating parameters on particle number emissions. *Energy Fuels* **2012**, *26*, 2014−2027.

(9) Barrientos, E. J.; Anderson, J. E.; Maricq, M. M.; Boehman, A. L. Particulate matter indices using smoke point for vehicle emissions with gasoline, ethanol blends, and butanol blends. *Combust. Flame* **2016**, *167*, 308−319.

(10) Maricq, M. M.; Szente, J. J.; Jahr, K. The impact of ethanol fuel blends on PM emissions from a light-duty GDI vehicle. *Aerosol Sci. Technol.* **2012**, *46*, 576−583.

(11) Karavalakis, G.; Short, D.; Vu, D.; Russell, R. L.; Asa-Awuku, A.; Jung, H.; Johnson, K. C.; Durbin, T. D. The impact of ethanol and isobutanol blends on gaseous and particulate emissions from two passenger cars equipped with spray-guided and wall-guided direct injection SI (spark ignition) engines. *Energy* **2015**, *82*, 168−179.

(12) Oh, H.; Bae, C. Effects on the injection timing on spray and combustion characteristics in a spray-guided DISI engine under lean-stratified operation. *Fuel* **2013**, *107*, 225−235.

(13) Maricq, M. M.; Szente, J. J.; Adams, J.; Tennison, P.; Rumpsa, T. Influence of mileage accumulation on the particle mass and number emissions of two gasoline direct injection vehicles. *Environ. Sci. Technol.* **2013**, *47*, 11890−11896.

(14) Chan, T. W.; Meloche, E.; Kubsh, J.; Rosenblatt, D.; Brezny, R.; Rideout, G. Evaluation of a gasoline particulate filter to reduce particle emissions from a gasoline direct injection vehicle. *SAE Int. J. Fuels Lubr.* **2012**, *5*, 1277−1290.

(15) Lambert, C. K.; Bumbaroska, M.; Dobson, D.; Hangas, J.; Pakko, J.; Tennison, P. Analysis of high mileage gasoline exhaust particle filters. *SAE Technical Paper* **2016**, *9*, 2016-01-0941.

(16) Mamakos, A.; Steininger, N.; Martini, G.; Dilara, P.; Drossinos, P. Cost effectiveness of particulate filter installation on direct injection gasoline vehicles. *Atmos. Environ.* **2013**, *77*, 16−23.

DOI: 10.1021/acs.est.7b05641
Environ. Sci. Technol. 2018, 52, 3275−3284

(17) Mamakos, A.; Martini, G.; Marotta, A.; Manfredi, U. Assessment of different technical options in reducing particle emissions from gasoline direct injection vehicles. *J. Aerosol Sci.* **2013**, *63*, 115−125.
(18) Chan, T. W.; Meloche, E.; Kubsh, J.; Brezny, R. Black carbon emissions in gasoline exhaust and a reduction alternative with a gasoline particulate filter. *Environ. Sci. Technol.* **2014**, *48*, 6027−6034.
(19) Choi, K.; Kim, J.; Ko, A.; Myung, C. L.; Park, S.; Lee, J. Size-resolved engine exhaust aerosol characteristics in a metal foam particulate filter for GDI light-duty vehicle. *J. Aerosol Sci.* **2013**, *57*, 1−13.
(20) Spiess, S.; Wong, K. F.; Richter, J. M.; Klingmann, R. Investigations of emissions control systems for gasoline direct injection engines with a focus on removal of particulate emissions. *Top. Catal.* **2013**, *56*, 434−439.
(21) Munoz, M.; Heeb, N. V.; Haag, R.; Honegger, P.; Zeyer, K.; Mohn, J.; Comte, P.; Czerwinski, J. Bioethanol blending reduces nanoparticle, PAH, and alkyl- and nitro-PAH emissions and the genotoxic potential of exhaust from a gasoline direct injection flex-fuel vehicle. *Environ. Sci. Technol.* **2016**, *50*, 11853−11861.
(22) Maikawa, C. L.; Zimmerman, N.; Rais, K.; Shah, M.; Hawley, B.; Pant, P.; Jeong, C. H.; Delgado-Saborit, J. M.; Volckens, J.; Evans, G.; Wallace, J. S.; Godri Pollitt, K. J. Murine precision-cut lung slices exhibit acute responses following exposure to gasoline direct injection engine emissions. *Sci. Total Environ.* **2016**, *568*, 1102−1109.
(23) Richter, H.; Howard, J. B. Formation of polycyclic aromatic hydrocarbons and their growth to soot-a review of chemical reaction pathways. *Prog. Energy Combust. Sci.* **2000**, *26*, 565−608.
(24) Kim, K. H.; Jahan, S. A.; Kabir, E.; Brown, R. J. C. A review of airborne polycyclic aromatic hydrcarbons (PAHs) and their human health effects. *Environ. Int.* **2013**, *60*, 71−80.
(25) Lundstedt, S.; White, P. A.; Lemieux, C. L.; Lynes, K. D.; Lambert, I. B.; Öberg, L.; Haglund, P.; Tysklind, M. Sources, fate, and toxic hazards of oxygenated polycyclic aromatic hydrocarbons (PAHs) at PAH-contaminated sites. *Ambio* **2007**, *36*, 475−485.
(26) Hu, S.; Herner, J. D.; Robertson, W.; Kobayashi, R.; Chang, M. C.; Huang, S. M.; Zielinska, B.; Kado, N.; Collins, J. F.; Rieger, P.; Huai, T.; Ayala, A. Emissions of polycyclic aromatic hydrocarbons (PAHs) and nitro—PAHs from heavy-duty diesel vehicles with DPF and SCR. *J. Air Waste Manage. Assoc.* **2013**, *63*, 984−996.
(27) Xia, W.; Zheng, Y.; He, X.; Yang, D.; Shao, H.; Remias, J.; Roos, J.; Wang, Y. Catalyzed gasoline particulate filter (GPF) performance: effect of driving cycle, fuel, catalyst coating. *SAE Tech. Pap. Ser.* **2017**, 2017-01-2366.
(28) Czerwinski, J.; Comte, P.; Heeb, N.; Mayer, A.; Hensel, V. Nanoparticle emissions of DI gasoline cars with/without GPF. *SAE Tech. Pap. Ser.* **2017**, 2017-01-1004.
(29) Quiros, D. C.; Zhang, S.; Sardar, S.; Kamboures, M. A.; Eiges, D.; Zhang, M.; Jung, H. S.; McCarthy, M. J.; Chang, M. C. O.; Ayala, A.; Zhu, Y.; Huai, T.; Hu, S. Measuring particulate emissions of light duty passenger vehicles using integrated particle size distribution (IPSD). *Environ. Sci. Technol.* **2015**, *49*, 5618−5627.
(30) Xue, J.; Quiros, D.; Wang, X.; Durbin, T. D.; Johnson, K. C.; Karavalakis, G.; Hu, S.; Huai, T.; Ayala, A.; Jung, H. S. Using a new inversion matrix for a fast-sizing spectrometer and a photo-acoustic instrument to determine suspended particulate mass over a transient cycle for light-duty vehicles. *Aerosol Sci. Technol.* **2016**, *50*, 1227−1238.
(31) Maricq, M. M.; Chase, R. E.; Podsiadlik, D. H.; Vogt, R. Vehicle exhaust particle size distributions: a comparison of tailpipe and dilution tunnel measurements. *SAE Tech. Pap. Ser.* **1999**, 1999-01-1461.
(32) Koczak, J.; Boehman, A.; Brusstar, M. Particulate emissions in GDI vehicle transients: An examination of FTP, HWFET, and US06 measurements. *SAE Tech. Pap. Ser.* **2016**, 2016-01-0992.
(33) Zhang, S.; McMahon, W. Particulate emissions for LEV II light-duty gasoline direct injection vehicles. *SAE Int. J. Fuels Lubr.* **2012**, *5*, 637−646.
(34) Cheng, Y.; Wang, J.; Zhuang, R.; Wu, N. Analysis of Combustion behavior during cold-start and warm-up process of SI gasoline engine. *SAE Tech. Pap. Ser.* **2001**, 2001-01-3557.
(35) Badshah, H.; Kittelson, D.; Northrop, W. Particle emissions from light-duty vehicles during cold-cold start. *SAE Int. J. Engines* **2016**, *9*, 1775−1785.
(36) Chen, L.; Liang, Z.; Zhang, X.; Shuai, S. Characterizing particulate matter emissions from GDI and PFI vehicles under transient and cold start conditions. *Fuel* **2017**, *189*, 131−140.
(37) Chan, T. W.; Saffaripour, M.; Liu, F.; Hendren, J.; Thomson, K. A.; Kubsh, J.; Brezny, R.; Rideout, G. Characterization of real-time particle emissions from a gasoline direct injection vehicle quipped with a catalyzed gasoline particulate filter during filter regeneration. *Emiss. Control Sci. Technol.* **2016**, *2*, 75−88.
(38) Saffaripour, M.; Chan, T. W.; Liu, F.; Thomson, K. A.; Smallwood, G. J.; Kubsh, J.; Brezny, R. Effect of drive cycle and gasoline particulate filter on the size and morphology of soot particles emitted from a gasoline-direct-injection vehicle. *Environ. Sci. Technol.* **2015**, *49*, 11950−11958.
(39) Maricq, M. M.; Szente, J. J.; Harwell, A. L.; Loos, M. J. Impact of aggressive drive cycles on motor vehicle exhaust PM emissions. *J. Aerosol Sci.* **2017**, *113*, 1−11.
(40) An, Y.-Z.; Pei, Y.-Q.; Qin, J.; Zhao, H.; Teng, S.-P.; Li, B.; Li, X. Development of a PAH (polycyclic aromatic hydrocarbon) formation model for gasoline surrogates and its application for GDI (gasoline direct injection) engine CFD (computational fluid dynamics) simulation. *Energy* **2016**, *94*, 367−379.
(41) International Agency for Research on Cancer. Working Group on the Evaluation of Carcinogenic Risks to Humans. Ingested nitrate and nitrite, and cyanobacterial peptide toxins. In *IARC Monographs on the Evaluation of Carcinogenic Risks to Humans*; IARC monographs on the evaluation of carcinogenic risks to humans; World Health Organisation: Geneva, Switzerland, 2010; Vol. *94*.
(42) Storey, J. M.; Lewis, S.; Szybist, J.; Thomas, J.; Barone, T.; Eibl, M.; Nafziger, E.; Kaul, B. Novel Characterization of GD engine exhaust for gasoline and mid-level gasoline-alcohol blends. *SAE Int. J. Fuels Lubr.* **2014**, *7*, 571−579.
(43) Andersson, J. T.; Achten, C. Time to say goodbye to the 16 EPA PAHs? Toward an up-to-date use of PACs for environmental purposes. *Polycyclic Aromat. Compd.* **2015**, *35*, 330−354.
(44) An, Y.-Z.; Teng, S.-P.; Pei, Y.-Q.; Qin, J.; Li, X.; Zhao, H. An experimental study of polycyclic aromatic hydrocarbons and soot emissions from a GDI engine fueled with commercial gasoline. *Fuel* **2016**, *164*, 160−171.
(45) Slavinskaya, N. A.; Riedel, U.; Dworkin, S. B.; Thomson, M. J. Detailed numerical modeling of PAH formation and growth in non-premixed ethylene and ethane flames. *Combust. Flame* **2012**, *159*, 979−995.
(46) Lea-Langton, A. R.; Ross, A. B.; Bartle, K. D.; Andrews, G. E.; Jones, J. M.; Li, H.; Pourkashanian, M.; Williams, A. Low temperature PAH formation in diesel combustion. *J. Anal. Appl. Pyrolysis* **2013**, *103*, 119−125.
(47) Brandenberger, S.; Mohr, M.; Grob, K.; Neukom, H. P. Contribution of unburned lubricating oil and diesel fuel to particulate emission from passenger cares. *Atmos. Environ.* **2005**, *39*, 6985−6994.
(48) Heeb, N. V.; Schmid, P.; Kohler, M.; Gujer, E.; Zennegg, M.; Wenger, D.; Wichser, A.; Ulrich, A.; Gfeller, U.; Honegger, P.; Zeyer, K.; Emmenegger, L.; Petermann, J. L.; Czerwinski, J.; Mosimann, T.; Kasper, M.; Mayer, A. Secondary effects of catalytic diesel particulate filters: conversion of PAHs versus formation of nitro-PAHs. *Environ. Sci. Technol.* **2008**, *42*, 3773−3779.

DOI: 10.1021/acs.est.7b05641
Environ. Sci. Technol. 2018, 52, 3275−3284